Thermodynamic analysis and mass spectra of heavy mesons via the generalized fractional Klein-Gordon equation

M. Abu-shady

Department of Mathematics and Computer Sciences, Faculty of Science, Menoufia University, Egypt.

H. M. Fath-Allah

Higher Institute of Engineering and Technology, Menoufia, Egypt.

Received 11 July 2024; accepted 11 November 2024

By employing the generalized fractional Nikiforov-Uvarov (GF-NU) method, we successfully derive solutions of the generalized fractional Klein-Gordon (GF-KG) equation for both the screened Kratzer and a specific class of Yukawa potentials. These solutions yield the generalized fractional energy eigenvalues across both the relativistic and non-relativistic domains. Furthermore, the corresponding generalized fractional eigenfunctions can be obtained. We employed the derived solutions to calculate the heavy-meson masses of Charmonium ($c\bar{c}$) and Bottomonium ($b\bar{b}$), along with those of heavy-light mesons ($c\bar{s}$, $c\bar{q}$, $b\bar{s}$, $b\bar{q}$). Notably, the Charmonium and Bottomonium masses were plotted as functions of the orbital and angular quantum numbers, reduced mass, and fractional parameter. Similarly, the heavy-light meson masses were plotted in relation to their orbital and angular quantum numbers. Additionally, a thermodynamic analysis of the heavy-light mesons was conducted. The obtained results demonstrate a high degree of concordance with established experimental data and the findings of other researchers

Keywords: The generalized fractional Kelin-Gordon; the screened Kratzer and a class of Yukawa potential; heavy and heavy-light meson.

DOI: https://doi.org/10.31349/RevMexFis.71.030801

1. Introduction

The Dirac and Klein-Gordon equations are key tools used to describe the motion of particles in the relativistic regime, with each equation applying to different types of particles based on their spin. The Klein-Gordon equation is used for spin-zero particles, like mesons, while the Dirac equation is applicable to spin-half particles, such as electrons [1,2].

Solving these equations precisely remains a significant challenge in nuclear and high-energy physics. The study of exactly solvable potentials, which dates back to the early days of quantum mechanics, has been of particular interest. Two notable examples of exact solutions to the Klein-Gordon equation are for the three-dimensional harmonic oscillator and the hydrogen atom [3,4].

To solve the Klein-Gordon equation, it's necessary to introduce a four-vector potential $V(r)$ and a scalar potential $S(r)$ that depend on space-time. These potentials, along with the four-vector linear momentum operator and the rest mass, allow for a more accurate description of particle behavior.

Research has shown that when the condition $S(r) = V(r)$ or $S(r) = -V(r)$ [5], is met, the Klein-Gordon equation yields the same energy spectrum.

Additionally, setting $S(r) = V(r) = 2\ V_1(r)$ results in non-relativistic energy bounds that align with the Schrödinger equation [6]. Recent studies have focused on finding solutions to the Klein-Gordon equation for different potentials [1,4,7].

For example, in one study, the Yukawa potential was used to solve the Klein-Gordon equation using the NU method, which provided energy eigenvalues in both relativistic and non-relativistic domains. The corresponding wave functions were expressed in terms of Laguerre polynomials.

This work contributed to calculating the masses of charmonium and bottomonium mesons [7]. In work of Berkdemir *et al.* [8], the modified Kratzer potential (MKP) has been the subject of substantial research in the literature by various writers [9,10].

Furthermore, by adding the screening parameter to the traditional Kratzer potential [11], Ikot et al. [12] presented the screened Kratzer potential (SKP). Edet *et al.* recently proposed the screened modified Kratzer potential [13].

Using this potential, the interatomic interactions in two-atom molecules were investigated. Here is the screened modified Kratzer potential (SMKP):

$$V_1(r) = d + \frac{f\ e^{-2\ \rho\ r}}{r^2} - \frac{g\ e^{-\rho\ r}}{r}. \tag{1}$$

Another interesting kind of potential model is the class of Yukawa potential (CYP), which has applications in atomic, nuclear, and condensed matter physics, among other fields of physics. The CYP manifests as the following

$$V_1(r) = \frac{-a}{r} + \frac{b\ e^{-\rho\ r}}{r} - \frac{c\ e^{-2\rho\ r}}{r^2}. \tag{2}$$

In order to provide more practical applications, employing two or more potentials has gained importance recently.

It is well known that potential models with more parameters typically provide a more accurate match to experimental data [14–16].

The SMKCYP is of the form

$$V_1(r) = d + \frac{f\, e^{-2\,\rho\, r}}{r^2} - \frac{g\, e^{-\rho\, r}}{r} - \frac{a}{r} + \frac{b\, e^{-\rho\, r}}{r} - \frac{c\, e^{-2\rho\, r}}{r^2}. \quad (3)$$

Asymptotic freedom and quark confinement are two essential components of strong interaction that these potentials should include [17]. Yukawa proposed the Yukawa potential as a useful non-relativistic potential to describe the strong nucleon interactions.

Finding solution of the KG and Schrӧdinger equations' approximate or exact solutions with a usual potential has been one of the most extensively researched issues in quantum mechanics during the past few decades [18, 19].

The last several decades of the 20th and 21st centuries have seen a considerable increase in the interest in fractional calculus (FC), among researchers. In Ref. [20], for the fractional Klein-Fock-Gordon (KFG) structure, which is extensively utilized in the particle and condensed matter physics, this work offers new waveforms and bifurcation analysis.

The one-dimensional KG equation for the generalized Hulthen potential was obtained using the CF-NU technique [21].

Abu-Shady and Kaabar recently presented a new definition for the fractional derivative known as the generalized fractional derivative (GFD) [22]. It can be said that the GFD definition is a more comprehensive type for the fractional derivative because it has greater characteristics than the previous definitions [23–26], from which the CFD can be constructed as a special case.

In Ref. [27], the researchers used a generalized fractional parametric NU method to solve the Schrödinger equation and calculate the mass of heavy quarkonium, specifically for Charmonium and Bottomonium.

In Ref. [28], Ikot *et al*., studied generalized Yukawa potentials and examined both relativistic and non-relativistic thermal properties, including the limit and scattering states of the Klein-Gordon equation for the Mobius square potential.

In Ref. [29], Inyang and colleagues investigated the masses and thermal characteristics of bottomonium and charmonium mesons.

In Ref. [30], the mass of charmonium was calculated using the asymptotic iteration method to solve the Schrödinger equation for quark-antiquark interactions.

Ref. [31] also applied the asymptotic iteration method to analytically solve the non-relativistic radial Schrödinger equation for a general interaction potential, using the Cornell potential and the Cornell plus harmonic potential as examples.

They obtained energy eigenvalues in three dimensions and used them to calculate charmonium mass spectra.

In Ref. [32], a relativistic potential model was used in momentum space to study the bottomonium spectrum. This model accounts for virtual pair production effects near decay thresholds, based on a one-gluon exchange interaction with a momentum-dependent screening factor. The model does not rely on non-relativistic approximations.

Ref. [33] discusses new theoretical findings on charmonium, focusing on "higher charmonium" states above the open-charm threshold, including the spectrum of these states, strong decays with open flavors, and the important effects of virtual decay loops in charmed meson pairs.

Research on thermodynamic properties is important in many areas of physics and chemistry. Quantum mechanical solutions, which provide the necessary information to describe quantum systems, are essential for understanding these properties.

Thermodynamic characteristics are especially useful in studying quark-gluon plasma and can provide valuable insights into the composition of strange quark matter, as discussed in Refs. [27, 34–36].

The aim of the paper is to obtain the generalized fractional energy eigenvalue and the generalized fractional wave function in two cases the relativistic and nonrelativistic domain by using the generalized fractional parametric NU method to solve the generalized fractional Kelin-Gordon equation which previous efforts did not take into account.

In nonrelativistic case, we evaluate the mass of heavy and heavy-light meson and thermodynamics properties of heavy-light meson $c\bar{s}$ under effect the angular quantum number and fractional factor which are compared with previous works.

The paper has the following structure: Section 2 reviews the (GF-NU) technique. The generalized fractional Kelin-Gordon equation is found in Sec. 3. Section 4 discusses the results. Section 5 presents the conclusion.

2. The generalized fractional Nikiforov-Uvarov (GF-NU) method

The parametric generalized fractional Nikiforov-Uvarov (NU) approach is presented using a generalized fractional derivative. Reference [37] provides an exact fractional form solution to the second-order parametric generalized differential equation.

$$D^{\alpha}[D^{\alpha}\psi(s)] + \frac{\overline{\tau}\,(s)}{\sigma(s)} D^{\alpha}\psi(s) \; + \frac{\overline{\sigma}(s)}{\sigma^2}\; \psi(s) = 0, \quad (4)$$

where the polynomials $\overline{\sigma}(s)$, $\sigma(s)$ and $\overline{\tau}\,(s)$ have degrees of 2α, 2α, and α.

By using GFD [22], we can write,

$$\mathrm{D}^{\alpha}[\psi(s)] = \frac{\Gamma(\beta)}{\Gamma(\beta-\alpha-1)} s^{1-\alpha} \acute{\psi}(s), \quad (5)$$

where, $\kappa = \Gamma(\beta)/\Gamma(\beta-\alpha-1)$

$$\mathrm{D}^{\alpha}[\mathrm{D}^{\alpha}[\psi(s)]] = \left(\frac{\Gamma\,(\beta)}{\Gamma\,(\beta-\alpha-1)}\right)^2 \times \left[(1-\alpha)\; s^{1-2\alpha} \acute{\psi}(s) + s^{2-2\alpha}\; \psi^{''}(s)\right], \quad (6)$$

where,

$$\pi(s)=\frac{D^{\alpha}\sigma(s)-\overline{\tau}(s)}{2}\pm\sqrt{\left(\frac{D^{\alpha}\sigma(s)-\overline{\tau}(s)}{2}\right)^{2}-\overline{\sigma}(s)+K\,\sigma(s)}\,,\tag{7}$$

and

$$\lambda=K+D^{\alpha}\pi(\mathrm{s}).\tag{8}$$

The polynomial of degree α is represented by $\pi(s)$,while λ remains constant. It is possible to find out whether the formula under the square root is square of the equation by looking at the values of K in the square-root of Eq. (7). By substituting K into Eq. (7), we establish

$$\tau(s)=\overline{\tau}(s)+2\pi(s).\tag{9}$$

Given that $\rho(s)>0$ and $\sigma(s)\ >0$, the derivative of τ needs to be negative [38]. This indicates that the solution is found. Should λ in Eq. (8) be

$$\lambda=\lambda_n=-nD^{\alpha}\,\tau-\frac{n(n-1)}{2}D^{\alpha}[D^{\alpha}\sigma(s)].\tag{10}$$

The hypergeometric type equation has a particular solution with degree α. Equation (11) has a solution which is the product of two independent parts

$$\psi(s)=\phi(s)y(s)\,,\tag{11}$$

where,

$$y_n(s)=\frac{B_n}{\rho(s)}(D^{\alpha})^{n}(\,\sigma(s))^{n}\,\rho_n(s),\tag{12}$$

$$D^{\alpha}[\sigma(s)\rho(s)]=\tau(s)\sigma(s)\,,\tag{13}$$

$$\frac{D^{\alpha}\phi(\mathrm{s})}{\phi(\mathrm{s})}=\frac{\pi(s)}{\sigma(s)}.\tag{14}$$

2.1. Second order parametric (GD) equation

The KG equation can be transformed into a second-order parametric generalized differential equation to provide the following general form. [30].

$$D^{\alpha}[D^{\alpha}\psi(s)]+\frac{\alpha_1-\alpha_2\,s^{\alpha}}{s^{\alpha}(1-\alpha_3\,s^{\alpha})}D^{\alpha}\psi(s)+\frac{-\,\xi_1\,s^{2\alpha}+\xi_2\,s^{\alpha}-\xi_3}{\left(s^{\alpha}\left(1-\alpha_3\,s^{\alpha}\right)\right)^{2}}\,\psi(s)=0,\tag{15}$$

$$\overline{\tau}(s)=\alpha_1-\alpha_2\,s^{\alpha},\tag{16}$$

$$\sigma(s)=s^{\alpha}\left(1-\alpha_3\,s^{\alpha}\right),\tag{17}$$

$$\bar{\sigma}(s)=-\,\xi_1\,s^{2\alpha}+\xi_2\,s^{\alpha}-\xi_3.\tag{18}$$

Substituting these into Eq. (7), we obtain

$$\pi=\alpha_4+\alpha_5 s^{\alpha}\pm\sqrt{(\alpha_6\ -\ \mathrm{K}\,\alpha_3)\,s^{2\alpha}+(\alpha_7+\mathrm{K})\ \,s^{\alpha}+\alpha_8},\tag{19}$$

where,

$$\alpha_4\ =\frac{1}{2}(\kappa\,\alpha-\alpha_1),\tag{20}$$

$$\alpha_5\ =\frac{1}{2}(\alpha_2--2\alpha_3\kappa\,\alpha),\tag{21}$$

$$\alpha_6\ =\alpha_5{}^{2}+\xi_1\,,\tag{22}$$

$$\alpha_7=2\alpha_4\alpha_5-\xi_2,\tag{23}$$

$$\alpha_8=\alpha_4{}^{\,2}+\ \xi_3.\tag{24}$$

In Eq. (19), the NU approach requires that the function under the square root be the square of a polynomial for reason

$$K=-(\alpha_7+2\,\alpha_3\alpha_8)\pm2\sqrt{\alpha_8\alpha_9},\tag{25}$$

where,

$$\alpha_9=\alpha_3\alpha_7+\alpha_3{}^{2}\alpha_8+\alpha_6.\tag{26}$$

If K in the form is negative

$$K=-(\alpha_7+2\,\alpha_3\alpha_8)-2\sqrt{\alpha_8\alpha_9},\tag{27}$$

for π to take shape

$$\pi=\alpha_4+\alpha_5 s^{\alpha}-[(\sqrt{\alpha_9}+\alpha_3\sqrt{\alpha_8})\;s^{\alpha}-\sqrt{\alpha_8}].\tag{28}$$

From Eqs. (16), (19) and (28), we get

$$\tau=\alpha_1+2\alpha_4-(\alpha_2--2\alpha_5)s^{\alpha}-[(\sqrt{\alpha_9}+\alpha_3\sqrt{\alpha_8})\;s^{\alpha}-\sqrt{\alpha_8}].\tag{29}$$

From Eqs. (2) and (26), we obtain,

$$D^{\alpha}\,\tau=\kappa\,[-\,\alpha\,(\alpha_2-2\alpha_5)-2\,\alpha(\sqrt{\alpha_9}+\alpha_3\sqrt{\alpha_8})\,]=\kappa\,[-2\,\alpha^{2}\alpha_3-2\,\alpha(\sqrt{\alpha_9}+\alpha_3\sqrt{\alpha_8})]<0.\tag{30}$$

From Eqs. (8), and (10), we obtain the generalized fractional energy eigenvalue equation.

$$n\kappa\alpha\alpha_2-(2n+1)\kappa\alpha\,\alpha_5+(2n+1)\kappa\alpha(\sqrt{\alpha_9}+\alpha_3\sqrt{\alpha_8})+n(n-1)\kappa^{2}\alpha^{2}\alpha_3+\alpha_7+2\alpha_3\alpha_8+2\sqrt{\alpha_8\alpha_9}=0.\tag{31}$$

when $\alpha=1=\beta$, implying that $\kappa=1$, we obtain The energy eigenvalue's classical equation as Ref. [40]

$$n\alpha_2-(2n+1)\;\alpha_5+(2n+1)(\sqrt{\alpha_9}+\alpha_3\sqrt{\alpha_8})+n(n-1)\alpha_3+\alpha_7+2\alpha_3\alpha_8+2\sqrt{\alpha_8\alpha_9}=0.\tag{32}$$

from Eq. (10), we obtain

$$\rho(s)=s^{\frac{\alpha_{10}-\alpha}{\kappa}}(1-\ \alpha_3\,s^{\alpha})^{\frac{\alpha_{11}}{\alpha\,\kappa\,\alpha_3}\;-\;\frac{\alpha_{10}}{\alpha\,\kappa}-\;\frac{1}{\kappa}}.\tag{33}$$

From Eq. (13), we get

$$y_n = P_n^{\left(\frac{\alpha_{10}-\alpha}{\kappa},\ \frac{\alpha_{11}}{\alpha\ \kappa\ \alpha_3} - \frac{\alpha_{10}}{\alpha\ \kappa} - \frac{1}{\kappa}\right)}(1 - \ 2\ \alpha_3\ s^{\alpha}), \quad (34)$$

where,

$$\alpha_{10} = \alpha_1 + 2\alpha_4 + 2\sqrt{\alpha_8}, \quad (35)$$

$$\alpha_{11} = \alpha_2 - -2\alpha_5 + 2\left(\sqrt{\alpha_9} + \alpha_3\sqrt{\alpha_8}\right). \quad (36)$$

The generalized fractional solution of the eigenfunction is obtained from Eq. (11)

$$\psi(s) = s^{\frac{\alpha_{12}}{\kappa}}\ (1 - \alpha_3 s^{\alpha})^{\frac{-\alpha_{13}}{\alpha\ \kappa\ \alpha_3} - \frac{\alpha_{12}}{\alpha\ \kappa}} \times P_n^{\left(\frac{\alpha_{10}-\alpha}{\kappa}, \frac{\alpha_{11}}{\alpha\ \kappa\ \alpha_3} - \frac{\alpha_{10}}{\alpha\kappa} - \frac{1}{\kappa}\right)}\ (1 - 2\alpha_3\ s^{\alpha}), \quad (37)$$

where, $P_n^{(\gamma,\delta)}$ are Jacobi polynomials.

$$\alpha_{12} = \alpha_4 + \sqrt{\alpha_8}, \quad (38)$$

$$\alpha_{13} = \alpha_5 - \ (\sqrt{\alpha_9} + \alpha_3\sqrt{\alpha_8}). \quad (39)$$

Some problems, in case $\alpha_3 = 0$.

$$\lim_{\alpha_3\to 0} P_n^{\left(\frac{\alpha_{10}-\alpha}{\kappa}, \frac{\alpha_{11}}{\alpha\kappa\alpha_3} - \frac{\alpha_{10}}{\alpha\kappa} - \frac{1}{\kappa}\right)}(1 - \alpha_3 s^{\alpha}) = L_n^{\frac{\alpha_{10}-\alpha}{\kappa}}\left(\frac{\alpha_{11}}{\alpha\ \kappa} s^{\alpha}\right), \quad (40)$$

$$\lim_{\alpha_3\to 0} (1-\alpha_3\ s^{\alpha})^{\frac{-\alpha_{13}}{\alpha\kappa\alpha_3} - \frac{\alpha_{12}}{\alpha\kappa}} = e^{\frac{\alpha_{13}}{\alpha\kappa} s^{\alpha}}, \quad (41)$$

Eq. (37), becomes

$$\psi(s) = s^{\frac{\alpha_{12}}{\kappa}} e^{\frac{\alpha_{13}}{\alpha\ k} s^{\alpha}} L_n^{\frac{\alpha_{10}-\alpha}{\kappa}}\left(\frac{\alpha_{11}}{\alpha\ \kappa} s^{\alpha}\right). \quad (42)$$

Associated Laguerre Polynomials are represented by L_n.

The second application of Eq. (27) in the subsequent scenario

$$K = -(\alpha_7 + 2\ \alpha_3\alpha_8) + 2\sqrt{\alpha_8\alpha_9}, \quad (43)$$

then, the generalized fractional eigenfunction becomes,

$$\psi(s) = s^{\frac{\alpha_{12}{}^*}{\kappa}}(1 - \ \alpha_3\ s^{\alpha})^{\frac{-\alpha_{13}{}^*}{\alpha\ \kappa\ \alpha_3} - \frac{\alpha_{12}{}^*}{\alpha\ \kappa}} \times P_n^{\left(\frac{\alpha_{10}{}^*-\alpha}{\kappa},\ \frac{\alpha_{11}{}^*}{\alpha\ \kappa\ \alpha_3} - \frac{\alpha_{10}{}^*}{\alpha\ k} - \frac{1}{\kappa}\right)} \times (1 - \ 2\ \alpha_3\ s^{\alpha}). \quad (44)$$

The generalized fractional solution of the energy eigenvalue becomes,

$$n\kappa\alpha\alpha_2 - 2n\kappa\alpha\ \alpha_5 + (2n+1)\kappa\alpha(\sqrt{\alpha_9} - \alpha_3\sqrt{\alpha_8}) + n(n-1)\kappa^2\alpha^2\alpha_3 + \alpha_7 + 2\alpha_3\alpha_8 - 2\sqrt{\alpha_8\alpha_9} + \kappa\alpha\ \alpha_5 = 0, \quad (45)$$

where,

$$\alpha_{10}{}^* = \alpha_1 + 2\alpha_4 - 2\sqrt{\alpha_8},$$

$$\alpha_{11}{}^* = \alpha_2 - 2\alpha_5 + 2\left(\sqrt{\alpha_9} - \alpha_3\sqrt{\alpha_8}\right),$$

$$\alpha_{12}{}^* = \alpha_4 - \sqrt{\alpha_8},$$

$$\alpha_{13}{}^* = \alpha_5 - \ (\sqrt{\alpha_9} - \alpha_3\sqrt{\alpha_8}). \quad (46)$$

3. Solving generalized fractional Kelin-Gordon with the screened modified Kratzer and a class of Yukawa potential model

The KG equation for a spinless particle for $\hbar = c = 1$ in N-dimensional space is as [41]

$$\left[-\nabla^2 + (M + S(r))^2 + \frac{(N+2l-1)(N+2l-3)}{4\,r^2}\right] \times \psi(r,\theta,\varphi) = \left[E_{nl} - V(r)\right]^2 \psi(r,\theta,\varphi), \quad (47)$$

where ∇^2 is laplacian, M is the reduce mass, E_{nl} is the energy spectrum $n,\ l$ are the radial and orbital angular momentum quantum number, or vibrational-rotational quantum number, respectively in quantum chemistry.

It is customary to write the wave function as follows in order for it to meet the boundary conditions:

$$\psi(r,\theta,\varphi) = \frac{R_{nl}}{r} Y_{lm}(\theta,\varphi). \quad (48)$$

The wavefunction's radial component would remain intact if the angular component were separated, as illustrated below.

$$\frac{d^2R(r)}{dr^2} + \Big[({E_{nl}}^2 - M^2) + V^2(r) - S^2(r) - 2(E_{nl}V(r) + M\ S(r)) - \frac{(N+2l-1)(N+2l-3)}{4\,r^2}\Big] R(r) = 0. \quad (49)$$

As a result, Eq. (49) becomes for equal vector and scalar potentials $V(r) = S(r) = 2V_1(r)$.

$$\frac{d^2R(r)}{dr^2} + \Big[({E_{nl}}^2 - M^2) - 2\ V_1(r)(E_{nl} + M) - \frac{(N+2l-1)(N+2l-3)}{4\,r^2}\Big]\ R(r) = 0. \quad (50)$$

From Eq. (3) and Eq. (50), we get

$$\frac{d^2R(r)}{dr^2} + \Bigg(({E_{nl}}^2 - M^2) - 2(E_{nl} + M)\Big[d - \frac{f\ e^{-2\rho\ r}}{r^2} - \frac{g\ e^{-\rho\ r}}{r} - \frac{a}{r} + \frac{be^{-\rho\ r}}{r} - \frac{c\ e^{-2\rho\ r}}{r^2}\Big] \times \frac{(N+2l-1)(N+2l-3)}{4\,r^2}\Bigg) R(r) = 0. \quad (51)$$

We provide the Greene-Aldrich approximation strategy (GAAS) [42] to address the centrifugal barrier in order to solve Eq. (51). For $\rho \ll 1$, this GAAS is a reliable approximation to the centrifugal term, and it becomes

$$\frac{1}{r^2} \approx \frac{\rho^2}{\left(1 - e^{-\rho\, r}\right)^2}. \tag{52}$$

Let

$$s = e^{-\rho\, r}, \tag{53}$$

$$\frac{d^2R(s)}{ds^2} + \frac{1-s}{s(1-s)}\frac{dR(s)}{ds} + \frac{1}{\left[s(1-s)\right]^2}\left[-\gamma_1 s^2 + \gamma_2 s - \gamma_3\right] R(s) = 0, \tag{54}$$

$$\gamma_1 = -\varepsilon + t_1, \qquad \gamma_2 = -2\,\varepsilon + t_2, \qquad \gamma_3 = -\varepsilon + t_3, \tag{55}$$

$$\varepsilon = \frac{{E_{nl}}^2 - M^2}{\rho^2},$$

$$t_1 = \frac{2(E_{nl}+M)\,d}{\rho^2} + 2(E_{nl}+M)\,f + \frac{2(E_{nl}+M)\,g}{\rho} - 2(E_{nl}+M)\,c - \frac{2(E_{nl}+M)\,b}{\rho},$$

$$t_2 = \frac{4(E_{nl}+M)\,d}{\rho^2} + \frac{2(E_{nl}+M)\,g}{\rho} - \frac{2(E_{nl}+M)\;a}{\rho} - \frac{2(E_{nl}+M)\;b}{\rho},$$

$$t_3 = \frac{2(E_{nl}+M)\,d}{\rho^2} - \frac{2(E_{nl}+M)\;a}{\rho} + \frac{l\,(l+1)}{4}.$$

We get the generalized fractional Kelin-Gordon equation

$$D^\alpha[D^\alpha R(s)] + \frac{1-s^\alpha}{s^\alpha(1-s^\alpha)}D^\alpha R(s) + \frac{-\gamma_1\; s^{2\alpha} + \gamma_2 s^\alpha - \gamma_3}{\left(s^\alpha(1-s^\alpha)\right)^2}R(s) = 0. \tag{56}$$

With the following parameters, we can obtain

$$\begin{aligned}
&\alpha_1 = 1, \qquad \alpha_2 = 1, \qquad \alpha_3 = 1, \qquad \alpha_4 = \frac{1}{2}(\kappa\,\alpha - 1), \qquad \alpha_5 = \frac{1}{2}(1 - 2\,\kappa\,\alpha),\\
&\alpha_6 = \frac{1}{4}\,(1-2\kappa\,\alpha)^2 - \varepsilon + t_1, \qquad \alpha_7 = \frac{1}{2}(\kappa\,\alpha-1)(1-2\kappa\,\alpha) + 2\varepsilon\, -\, t_2, \qquad \alpha_8 = \frac{1}{4}(\kappa\,\alpha-1)^2 - \varepsilon + \, t_3,\\
&\alpha_9 = \frac{1}{4}\kappa^2\,\alpha^2\; + t_1 - t_2 + t_3, \qquad \alpha_{10} = \kappa\,\alpha + 2\sqrt{\frac{1}{4}(\kappa\,\alpha-1)^2\; - \varepsilon + t_3},\\
&\alpha_{11} = 2\kappa\,\alpha + 2\left(\sqrt{\frac{1}{4}\kappa^2\,\alpha^2\; + t_1 - t_2 + t_3} + \sqrt{\frac{1}{4}(\kappa\,\alpha-1)^2 - \varepsilon + t_3}\right),\\
&\alpha_{12} = \frac{1}{2}(\kappa\,\alpha - 1) + \sqrt{\;\frac{1}{4}(\kappa\,\alpha-1)^2\; - \varepsilon + t_3},\\
&\alpha_{13} = \frac{1}{2}(1-2\kappa\,\alpha) - \left(\sqrt{\frac{1}{4}\kappa^2\,\alpha^2\; + t_1 - t_2 + t_3} + \sqrt{\frac{1}{4}(\kappa\,\alpha-1)^2\; - \varepsilon + t_3}\right),
\end{aligned} \tag{57}$$

the generalized fractional of the energy eigenvalue is obtained

$$\varepsilon = \left(t_3 + \frac{1}{4}(\kappa\,\alpha-1)^2\right) - \left(\frac{t_1 - t_3 - \left(\left(n+\frac{1}{2}\right)\kappa\,\alpha + \sqrt{\frac{1}{4}\kappa^2\,\alpha^2\; + t_1 - t_2 + t_3}\right)^2}{2\left(\left(n+\frac{1}{2}\right)\kappa\,\alpha + \sqrt{\frac{1}{4}\kappa^2\,\alpha^2\; + t_1 - t_2 + t_3}\right)}\right)^2. \tag{58}$$

The generalized fractional wave function

$$\psi(s) = A s^{\frac{\frac{1}{2}(k\alpha-1)+\sqrt{\frac{1}{4}(\kappa\alpha-1)^2-\varepsilon+t_3}}{\kappa}}(1+s^\alpha)^{\frac{\frac{1}{2}\kappa\alpha+\sqrt{\frac{1}{4}\kappa^2\alpha^2+t}}{\kappa\alpha}}P_n^{\left(\frac{-\alpha+\kappa\alpha+2\sqrt{\frac{1}{4}(\kappa\alpha-1)^2-\varepsilon+t_3}}{\kappa\alpha},\frac{\kappa\alpha+2\sqrt{\frac{1}{4}\kappa^2\alpha^2+t}}{\kappa\alpha}-\frac{1}{\kappa}\right)}(1+2s^\alpha), \tag{59}$$

where $t = t_1 - t_2 + t_3$.

We obtain on the generalized fractional of the energy eigenvalue and eigenfunction in the non-relativistic case, $M + E_{nl} \to (2\mu/\hbar)$ and $M - E_{nl} \to -E_{nl}$ where μ is reduced mass

$$E_{nl} = \frac{\rho^2}{2\mu}(t_3 + \frac{1}{4}(\kappa\alpha - 1)^2) - \frac{\rho^2}{2\mu}\left(\frac{t_1 - t_3 - \left(\left(n+\frac{1}{2}\right)\kappa\alpha + \sqrt{\frac{1}{4}\kappa^2\alpha^2 + t_1 - t_2 + t_3}\right)^2}{2\left(\left(n+\frac{1}{2}\right)\kappa\alpha + \sqrt{\frac{1}{4}\kappa^2\alpha^2 + t_1 - t_2 + t_3}\right)}\right)^2, \tag{60}$$

$$R(s) = Ns^{\frac{\frac{1}{2}(k\alpha-1)+\sqrt{\frac{1}{4}(k\alpha-1)^2-\frac{2\mu E}{\rho^2}+t_3}}{\kappa}}(1+s^\alpha)^{\frac{\frac{1}{2}\kappa\alpha+\sqrt{\frac{1}{4}\kappa^2\alpha^2+t}}{\kappa\alpha}}$$
$$\times P_n^{\left(\frac{-\alpha+\kappa\alpha+2\sqrt{\frac{1}{4}(\kappa\alpha-1)^2-\frac{2\mu E}{\rho^2}+t_3}}{\kappa\alpha},\frac{\kappa\alpha+2\sqrt{\frac{1}{4}\kappa^2\alpha^2+t}}{k\alpha}-\frac{1}{\kappa}\right)}(1+2s^\alpha), \tag{61}$$

where,

$$t_1 = \frac{4\ \mu d}{\rho^2} + 4\mu f + \frac{4\mu g}{\rho} - 4\mu c - \frac{4\mu b}{\rho}, \quad t_2 = \frac{8\ \mu d}{\rho^2} + \frac{4\mu\ g}{\rho} - \frac{4\mu\ a}{\rho} - \frac{4\mu b}{\rho}, \quad t_3 = \frac{4\mu d}{\rho^2} - \frac{4\mu\ a}{\rho} + \frac{l\,(l+1)}{4}. \tag{62}$$

4. Results and discussion

4.1. Special case

The special case is obtained by taking ($\alpha = \beta = 1$) and $\kappa = 1$, we obtain the energy and the eigenfunction in the non-relativistic case

$$E = \frac{\rho^2}{2\ \mu}t_3 - \frac{\rho^2}{2\ \mu}\left(\frac{t_1 - t_3 - \left(\left(n+\frac{1}{2}\right) + \sqrt{\frac{1}{4}\ + t_1 - t_2 + t_3}\right)^2}{2\left(\left(n+\frac{1}{2}\right) + \sqrt{\frac{1}{4}\ + t_1 - t_2 + t_3}\right)}\right)^2, \tag{63}$$

$$R(s) = Ns^{\sqrt{-\frac{2\mu\ E}{\rho^2}+\ t_3}}(1+s)^{\frac{1}{2}+\sqrt{\frac{1}{4}+t}}P_n^{\left(\sqrt{-\frac{2\mu\ E}{\rho^2}+t_3},2\sqrt{\frac{1}{4}+t}\right)}(1+2s). \tag{64}$$

4.2. Mass of heavy and heavy-light mesons

To calculate the mass of heavy and heavy light mesons, the following the equation is used

$$M = m_1 + m_2 + E_{nl}, \tag{65}$$

$$M = m_1 + m_2 + \frac{\rho^2}{2\mu}\left(t_3 + \frac{1}{4}(\kappa\alpha - 1)^2\right) - \frac{\rho^2}{2\mu}\left(\frac{t_1 - t_3 - \left[\left(n+\frac{1}{2}\right)\kappa\alpha + \sqrt{\frac{1}{4}\kappa^2\ \alpha^2 + t_1 - t_2 + t_3}\right]^2}{2\left[\left(n+\frac{1}{2}\right)\kappa\alpha + \sqrt{\frac{1}{4}\kappa^2\alpha^2 + t_1 - t_2 + t_3}\right]}\right)^2. \tag{66}$$

In Table I, we determined the mass of $c\bar{c}$ is for 1S, 2S, 3S, 4S, 1P, 2P, 1D, and 2D. Ref. [7] provides the charm quark mass in numerical form.

By adding experimental data to algebraic equations, the parameters of Eq. (66) were determined where (charm mass $m_c = 1.209$ GeV, the parameters of the potential $d = 1$ GeV, $c = -10$ GeV^{-1}, $b = -0.5$, $a = 0.947$, $g = 0.02$, $f = -9.838$, the fractional parameters $\alpha = 0.3$, $\beta = 0.6$, $\rho = 0.04$ GeV).

Compared to previous studies, we achieved successful results. Additionally, the 1S and 1P states are close in comparison with the experimental results. Our calculation resulted in a total error of 0.017475%. In Ref. [7], the researchers used the Nikiforov–Uvarov method to solve the Klein-Gordon equation for the Yukawa potential.

They found the energy eigenvalues in both relativistic and non-relativistic domains, using the Laguerre polynomial to calculate the associated eigenfunction. Their findings were used to determine the mass of the charmonium heavy meson. Their total error was 0.2681%. In Ref. [30], the mass of charmonium was calculated using the asymptotic iteration method to solve the Schrödinger equation for the quark-antiquark potential.

The total error for this calculation was 0.13268%. Reference [31] used the same method to solve the non-relativistic radial Schrödinger equation with the Cornell and Cornell plus harmonic potentials. The energy eigenvalues were calculated in three dimensions, and they applied these results to determine the mass spectra of charmonium. The error from our calculation was 0.0478%.

TABLE I. Mass spectra of $c\bar{c}$ in (GeV) (charm mass $m_c = 1.209$ GeV, the parameters of the potential $d = 1$ GeV, $c = -10$ GeV^{-1}, $b = -0.5$, $a = 0.947$, $g = 0.02$, $f = -9.838$, fractional parameters $\alpha = 0.3, \beta = 0.6$, $\rho = 0.04$ GeV).

State	P.W	[7]	[30]	[31]	Exp. [43]	Total error of each state
1S	3.096	3.096	3.078	3.096	3.096	0
2S	3.685	3.686	4.187	3.686	3.686	0.0002
1P	3.525	3.527	3.514	3.214	3.525	0
2P	3.872	3.687	4.143	2.773	3.773	0.0262
3S	3.949	4.040	5.297	4.275	4.040	0.0225
4S	4.089	4.360	6.407	4.865	4.263	0.0408
1D	3.848	3.098	3.752	3.412	3.770	0.0295
2D	4.036	3.976	-	-	4.159	0.0295
Total error	0.017475	0.2681	0.13268	0.0478	-	-

TABLE II. Mass spectra of $b\bar{b}$ in (GeV) (bottom mass $m_b = 4.623$ GeV, the parameters of potential $d = 1$ GeV, $c = -10$ GeV^{-1}, $b = -0.5$, $a = 0.4118$, $g = 0.02$, $f = -9.894$, the fractional parameters $\alpha = 0.2$, $\beta = 0.6$, $\rho = 0.1$ GeV).

State	P.W	[44]	[31]	[45]	[46]	[30]	[47]	Exp. [48]	Total error of each state
1S	9.444	9.515	9.460	9.461	9.460	9.510	9.510	9.444	0
2S	10.044	10.018	10.023	10.023	10.023	10.627	10.038	10.023	0.0020
1P	9.900	-	9.492	9.608	9.619	9.862	9.862	9.900	0
2P	10.304	10.09	10.038	10.110	10.114	10.944	10.396	10.260	0.0042
3S	10.388	10.441	10.585	10.365	10.355	11.726	10.566	10.355	0.0031
4S	10.604	10.858	11.148	10.588	10.567	12.834	11.094	10.579	0.0023
1D	10.345	-	9.551	9.841	9.864	10.214	10.214	10.161	0.0181
Total error	0.0042	0.0083	0.0286	0.0112	0.0106	0.0835	0.0142		

The mass of $b\bar{b}$ for the following states: 1S, 2S, 3S, 4S, 1P, 2P, and 1D is found in Table II. We take the numerical value of 4.623 GeV for bottom mass m_b, respectively, from Ref. [30].

Then, by combining the solution of algebraic equations with experimental data, the free parameters of Eq. (66) were found where the parameters of the potential $d = 1$ GeV, $c = -10$ GeV^{-1},$b = -0.5$, $a = 0.4118$, $g = 0.02$, $f = -9.894$, the fractional parameters $\alpha = 0.2$, $\beta = 0.6$, $\rho = 0.1$ GeV.

Our results show a good agreement with previous studies, and there is a close match with experimental data. Our total error was 0.0042%. In Refs. [30, 31], the errors were 0.0835% and 0.0286%, respectively.

In Ref. [44], an analytical solution to the radial Schrödinger equation was obtained using a series expansion approach with a generalized anharmonic Cornell potential. The mass spectra for bottomonium were calculated with an error of 0.0083%.

Reference [45] solved the Schrödinger equation with the Killingbeck potential and an inversely quadratic potential, obtaining energy eigenvalues and mass spectra for heavy-light mesons. The error in this calculation was 0.0112%.

Reference [46] used the NU method to solve the N-dimensional Schrödinger equation with a temperature-dependent Cornell potential. The energy eigenvalues and wave functions were determined at zero temperature, and the bottomonium mass at higher temperatures was examined. The error for this study was 0.0106%.

Reference [47] calculated the energy eigenvalues and eigenfunctions for the quark-antiquark interaction potential using the power series method. Their total error was 0.0142%.

Table III, by using Eq. (66), we were able to determine the mass of $c\bar{s}$ where charm mass $m_c = 1.209$ GeV, strange mass $m_{\bar{s}} = 0.419$ GeV, the parameters of the potential $d = 1$ GeV, $c = -10$ GeV^{-1}, $b = -0.5$, $a = 2.019$, $g = 0.02$, $f = -9.996$, the fractional parameters $\alpha = \beta = 0.6$, $\rho = 0.18$ GeV.

Our results were better than those in recent studies, [31, 45, 49–52], and the total error was 0.0028%. In comparison, the errors in Refs. [31, 45] were 0.06757% and 0.020925%.

Reference [49] used the Rosen-Morse potential to study the thermodynamic properties of heavy mesons. The total error was 0.128725%.

TABLE III. Mass spectra of $c\bar{s}$ in (GeV) (charm mass $m_c = 1.209$ GeV, strange mass $m_{\bar{s}} = 0.419$ GeV, the parameters of the potential $d = 1$ GeV, $c = -10$ GeV^{-1}, $b = -0.5$, $a = 2.019$, $g = 0.02$, $f = -9.996$, the fractional parameters $\alpha = \beta = 0.6$, $\rho = 0.18$ GeV).

State	P.W	[45]	[31]	[49]	[50]	[51]	[52]	Exp. [48]
1S	2.067	1.969	2.512	1.969	2.075	2.067	2.076	2.067
2S	2.708	2.709	2.709	2.318	2.720	2.708	2.636	2.708
1P	2.512	2.601	2.649	2.126	2.537	2.512	2.515	2.512
2P	2.847	2.876	2.860	-	3.119	2.857	3.019	-
3S	2.878	2.913	2.906	2.667	3.236	2.935	3.061	-
4S	2.897	2.998	3.102	-	3.664	3.041	3.244	-
1D	2.827	2.862	2.859	2.374	2.950	2.812	2.831	2.860
Total error	0.0028	0.020925	0.06757	0.128725	0.01237	0.0041	0.0104	

TABLE IV. Mass spectra of $b\bar{s}$ in (GeV) (bottom mass $m_b = 4.623$ GeV, strange mass $m_{\bar{s}} = 0.419$ GeV, the parameters of the potential $d = 1$ GeV, $c = -10$ GeV^{-1}, $b = -0.5$, $a = 1.660$, $g = 0.02$, $f = -9.590$, the fractional parameters $\alpha = 0.3$, $\beta = 0.6$, $\rho = 0.1$ GeV).

State	P.W	[51]	[31]	[52]	[50]	[53]	[54]	ExP. [48]
1S	5.403	5.403	5.415	5.401	5.404	5.370	5.403	5.403
2S	6.039	5.942	6.819	6.168	5.988	5.971	5.952	-
1P	5.836	5.836	5.830	5.850	5.844	5.838	5.838	5.836
2P	6.243	6.066	6.786	6.380	6.343	6.254	6.233	-
3S	6.339	6.104	8.225	6.544	6.473	-	6.425	-
4S	6.500	6.174	9.629	6.756	6.878	-	6.863	-
1D	6.227	6.059	6.264	6.179	6.200	6.117	6.181	-
2D	6.451	-	-	6.604	6.635	6.450	6.626	-
Total error	-	-	0.0016	0.0013	0.0007	0.0032	0.00015	-

In Ref. [50], the quasipotential technique was used to calculate the masses of heavy-light mesons, with an error of 0.01237%. Ref. [51] applied the generalized Cornell potential model to solve the Dirac equation, and their error was 0.0041%.

Reference [52] solved the Klein-Gordon equation analytically using a combination of linear and modified Yukawa potentials. Their total error was 0.0104%.

In Table IV, we were able to calculate the mass of $b\bar{s}$ by using Eq. (66), where bottom mass $m_b = 4.623$ GeV, strange mass $m_{\bar{s}} = 0.419$ GeV, the parameters of the potential $d = 1$ GeV, $c = -10$ GeV^{-1}, $b = -0.5$, $a = 1.660$, $g = 0.02$, $f = -9.590$, the fractional parameters $\alpha = 0.3$, $\beta = 0.6$, $\rho = 0.1$ GeV.

These results were better than the latest studies (Refs. [31, 50–54]), and the error was 0.0016%. The errors in Refs. [31, 50, 52] were 0.0007%, 0.0013%, and 0.0032%, respectively.

In Ref. [53], a relativistic quark model was used to determine the mass spectra of heavy-light mesons, and the error was 0.0032%. Reference [54] used the relativistic independent quark model to study the B and B_s mesons, with an error of 0.00015%.

The mass of $c\bar{q}$ was found in Table V and by using Eq. (66), where charm mass $m_c = 1.209$ GeV, $m_{\bar{q}=\bar{u},\bar{d}} = 0.46$ GeV, the parameters of the potential $d = 1$ GeV, $c = -10$ GeV^{-1}, $b = -0.5$, $a = 1.773$, $g = 0.02$, $f = -9.556$, the fractional parameters $\alpha = 0.3$, $\beta = 0.6$, $\rho = 0.13$, GeV.

The current results surpass those in Refs. [52, 55–57], with a total error of 0.00583%. The results are in good agreement with the experimental data. We found the total error in Ref. [52] was 0.00583$\%$.

Reference [55], the authors presents a detailed analysis of the masses of the ground, orbitally, and radially excited states of the D-meson within the context of the screened potential model with the Gaussian wave-function.

The Hamiltonian includes relativistic adjustment to the kinetic energy term $O(p^{10})$ and $o(1/m)$ correction to the potential energy term. The spin-hyperfine, spin-orbit and tensor interactions integrating the effect of mixing are applied to derive the pseudoscalar, vector and radially and orbitally excited meson masses. Total error in Ref. [55] was 0.026$\%$.

In Ref. [56], the authors compute the excited charm and charm-strange meson characteristics. They compute their masses and wave functions, which are required to compute radiative transition partial widths, by using the relativized quark model. Total error in Ref. [56] was 0.139$\%$.

In Ref. [57], a comparison study of the decay properties and spectroscopy of the D-meson is carried out between the Gaussian and hydrogenic wave functions, in the framework of the phenomenological quark-antiquark potential (Coulomb plus power) model.

TABLE V. Mass spectra of $c\overline{q}$ in (GeV) (charm mass $m_c = 1.209$ GeV, $m_{\overline{q}} = 0.46$ GeV, the parameters of the potential $d = 1$ GeV, $c = -10$ GeV^{-1}, $b = -0.5$, $a = 1.773$, $g = 0.02$, $f = -9.556$, the fractional parameters $\alpha = 0.3$, $\beta = 0.6$, $\rho = 0.13$ GeV).

State	P.W	[52]	[55]	[56]	[57]	Exp. [58]
1S	1.975	1.978	1.975	2.000	1.973	1.975
2S	2.613	2.665	2.424	3.628	2.586	2.613
1P	2.434	2.434	2.448	2.473	2.448	2.434
2P	2.829	2.953	2.977	2.948	2.949	-
3S	2.907	3.074	3.118	3.100	3.104	-
4S	3.059	3.341	3.512	3.490	3.510	-
1D	2.841	2.783	2.777	2.830	2.768	-
2D	3.046	3.132	3.242	3.229	3.207	-
1F	3.108	3.009	3.048	-	-	-
Total error	-	0.00583	0.026	0.139	0.00566	

TABLE VI. Mass spectra of $b\overline{q}$ in (GeV) (bottom mass $m_b = 4.623$ GeV, $m_{\overline{q}} = 0.46$ GeV, the parameters of the potential $d = 1$ GeV, $c = -10$ GeV^{-1}, $b = -0.5$, $a = 1.754$, $g = 0.02$, $f = -9.532$, fractional parameters $\alpha = 0.3$, $\beta = 0.6$, $\rho = 0.11$ GeV).

State	P.W	[31]	[52]	[59]	[60]	Exp. [48]
1S	5.313	5.325	5.314	5.314	5.371	5.313
2S	5.970	6.413	5.924	5.951	5.933	5.971
1P	5.734	5.723	5.747	5.779	5.777	5.734
2P	6.175	6.486	6.100	6.307	6.197	-
3S	6.289	7.501	6.214	6.425	6.355	-
4S	6.464	8.589	6.474	6.846	6.703	-
1D	6.146	6.131	6.035	6.104	6.110	-
2D	6.398	-	6.273	6.571	-	-
Total error	0.000055	0.026033	0.0033	0.0037	0.0082	-

The spin-hyperfine, spin-orbit, and tensor interactions are used to obtain the pseudoscalar and vector meson masses with a mixing effect. Total error in Ref. [57] was 0.00566%.

The mass of $b\overline{q}$ was found in Table VI and by using Eq. (66), where bottom mass $m_b = 4.623$ GeV, $m_{\overline{q}=\overline{u},\overline{d}} = 0.46$ GeV, the parameters of the potential $d = 1$ GeV, $c = -10$ GeV^{-1}, $b = -0.5$, $a = 1.754$, $g = 0.02$, $f = -9.532$, the fractional parameters $\alpha = 0.3$, $\beta = 0.6$, $\rho = 0.11$ GeV.

The current results show a significant improvement over the latest Refs. [31,52,59,60], and there is a close match with experimental data. In our paper total error was 0.000055%.

In Refs. [31, 52], the total error were 0.02633% and 0.0033%. The masses of the ground, orbitally, and radially excited states are computed in Ref. [59], driven by the recent LHCb observations of the B and B_s meson states.

The Hamiltonian now includes $O(1/m)$ and $O(p^{10})$ relativistic corrections to the potential and kinetic energy terms. The employed screening potential is solved using the Gaussian wave function.

We are able to correlate some recently discovered states with B and B_s mesons by constructing the Regge trajectories using the predicted masses. We evaluated total error of Ref. [59] was 0.0037%.

In Ref. [60], inspired by the latest studies of the meson states of B and B_s properties of bottom and bottom-strange mesons are calculated in two relativized quark models. Model masses and wavefunctions are used to predict the rates of radiation transition. We found that total error of Ref. [60] was 0.0082%.

In this study, we analyzed the mass spectra of charmonium and bottomonium systems by plotting them with the reduced mass for different fractional parameters α and β. As shown in Figs. 1-5, for the orbital angular momentum quantum numbers a) $l = 0$ and b) $l = 1$, the mass spectra decrease with reduced mass, consistent with Ref. [52].

We also observed that the mass spectra increase as the orbital angular momentum quantum number l increases.

Furthermore, the mass spectra increase with higher values of the fractional parameters α and β. In Figs. 2-6, for a) $l = 0$ and b) $l = 1$, we plotted the charmonium and bottomonium mass spectra with the principal quantum number n for various values of α and β.

The results show that the mass spectra grow with n, which is consistent with Ref. [52].

Additionally, the mass spectra increase with both the orbital angular momentum quantum number l and the fractional

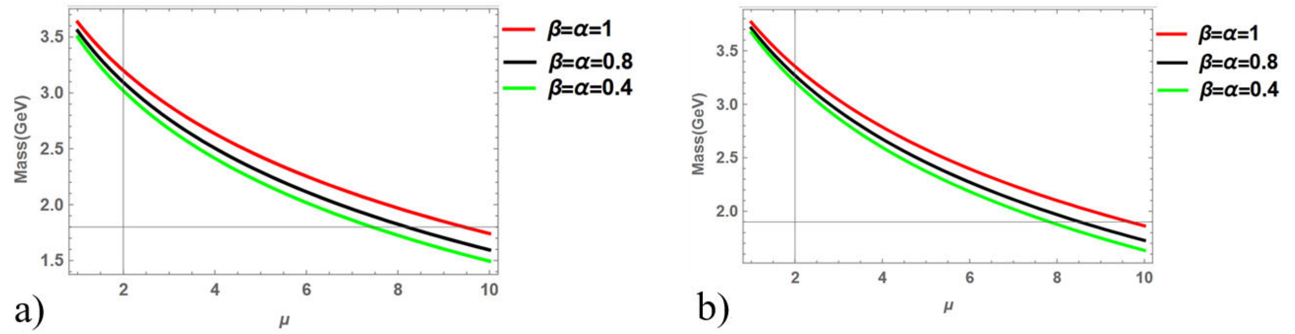

FIGURE 1. The mass spectra of Charmonium with reduced mass at different values of the fractional parameters α, β at the orbital angular momentum quantum number a) $l = 0$, b) $l = 1$.

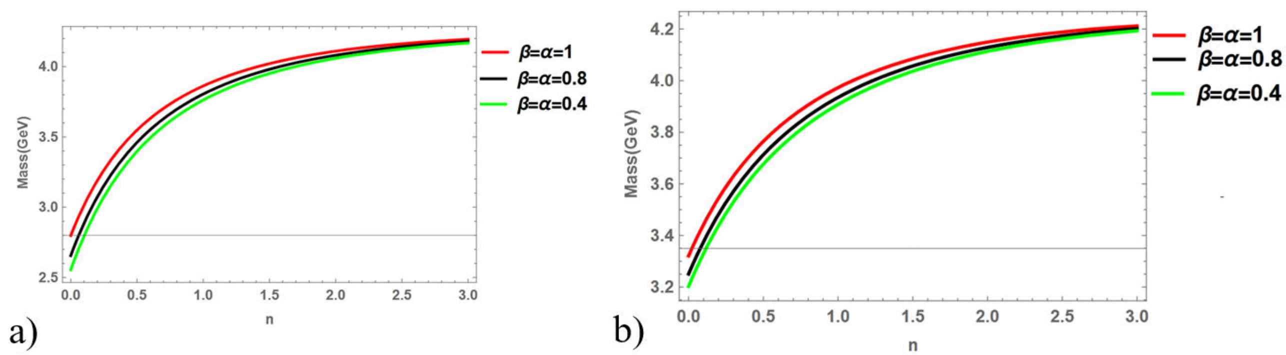

FIGURE 2. The mass spectra of Charmonium with n at different values of the fractional parameters α, β at the orbital angular quantum number a) $l = 0$, b) $l = 1$.

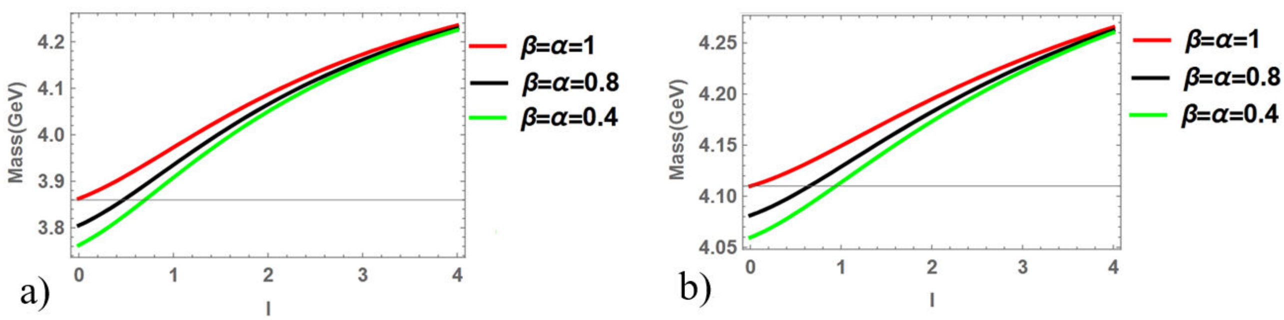

FIGURE 3. The mass spectra of Charmonium with the orbital angular momentum quantum number l at different of the fractional paramteres α, β at the principle quantum number a) $n = 1$, b) $n = 2$.

parameters α and β. In Figs. 3 and 7, for a) $n = 1$ and b) $n = 2$, we plotted the mass spectra of charmonium and bottomonium with l for different α and β values.

The results confirm that the mass spectra increase with l, and they also grow as α and β increase. When plotting charmonium and bottomonium mass spectra with α for different l values in Figs. 4, 8, we found that the mass spectra increase with α and rise further with higher l values.

In Fig. 9, for a) $\alpha = \beta = 1$ and b) $\alpha = \beta = 0.4$, we plotted the mass spectra of cs^-, cq^-, bs^-, and bq^- with n. We observed that the mass of the heavy-light mesons increases with n, and the mass spectra grow as α and β increase.

Finally, in Fig. 10, for a) $\alpha = \beta = 1$ and b) $\alpha = \beta = 0.4$, we plotted the mass spectra of cs^-, cq^-, bs^-, and bq^- against l. The results indicate that the mass of the heavy-light mesons increases with l, and the mass spectra also increase as α and β grow.

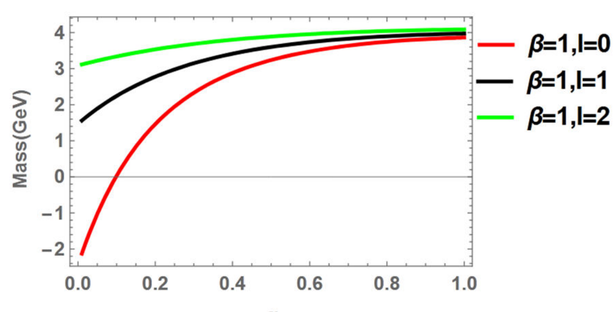

FIGURE 4. The mass spectra of Charmonium with factor parameter α at different of orbital angular momentum quantum number l.

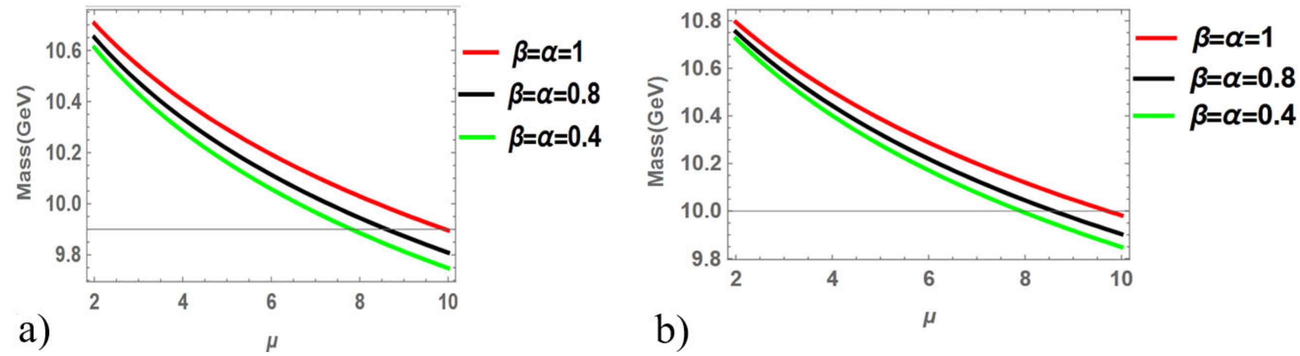

FIGURE 5. The mass spectra of Bottomonium with reduced mass at different values of the fractional parameters α, β at the orbital angular momentum quantum number a) $l = 0$, b) $l = 1$.

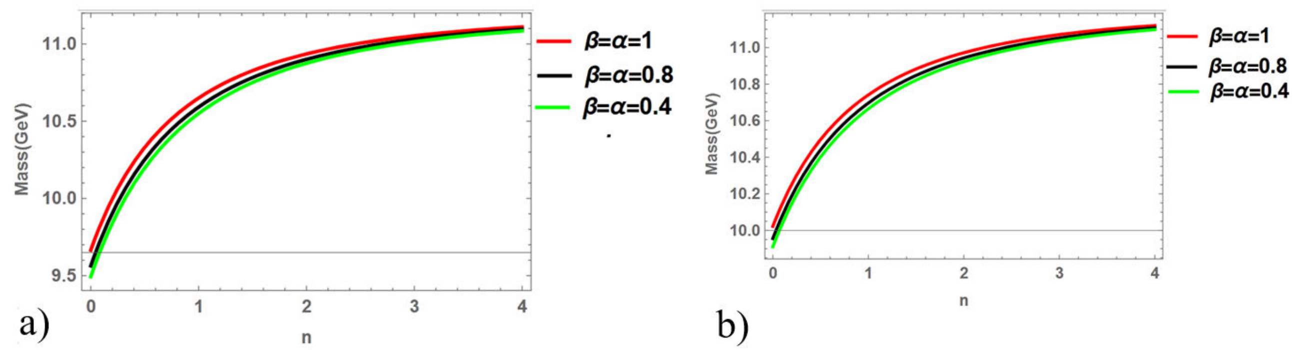

FIGURE 6. The mass spectra of Bottomonium with the principle quantum number n at different values of the fractional parameters α, β at the orbital angular momentum quantum number a) $l = 0$, b) $l = 1$.

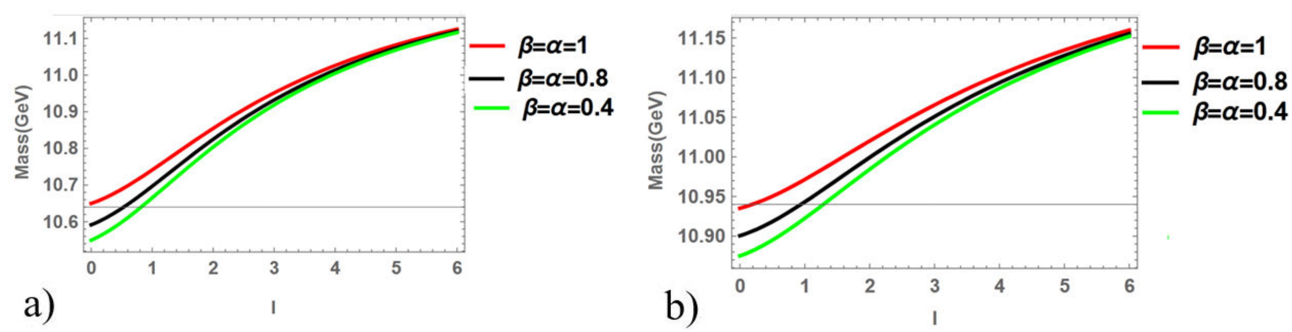

FIGURE 7. The mass spectra of Bottomonium with the orbital angular momentum quantum number l at different of the fractional parameters α, β at the principle quantum number a) $n = 1$, b) $n = 2$.

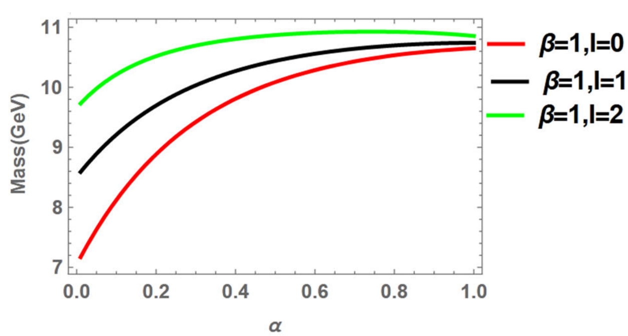

FIGURE 8. The mass spectra of Bottomonium with factor parameter α at different of the orbital angular momentum quantum number l.

4.3. Thermodynamics properties of heavy light meson

Using the resultant Eq. (66), the thermodynamic properties for the potential model are computed. The partition function can yield the thermodynamic characteristics of a quantum mechanical system, as $Z(\beta_s) = \sum_{n=0}^{\lambda} e^{-\beta_s E_n}$ where T is the system's absolute temperature, K is the Boltzmann constant, and $\beta_s = 1/K\,T$ and where λ is the quantum number with the highest upper bound obtained from the numerical solution of $dE_n/dn = 0$, It is possible to substitute the integral in Eq. (67) for the summation in the classical limit.

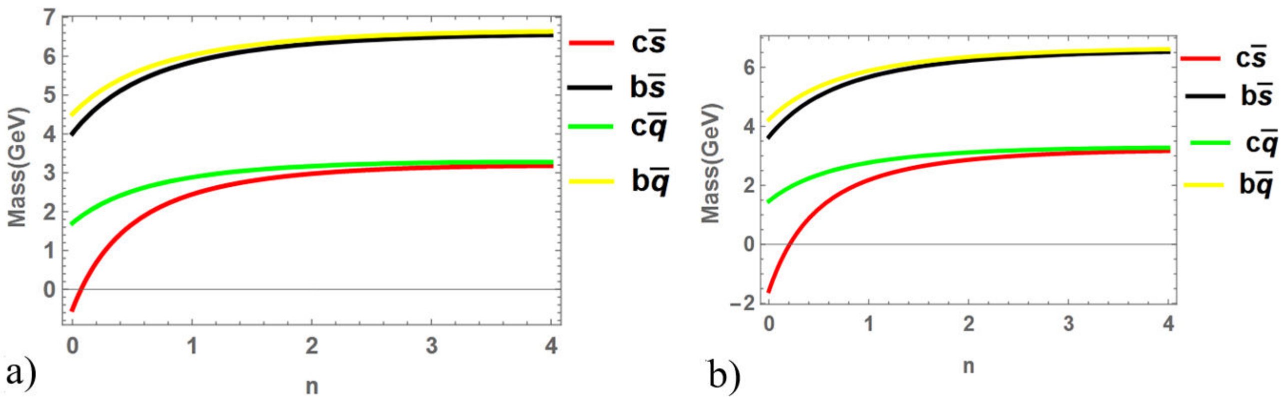

FIGURE 9. The mass spectra of $c\overline{s}$, $c\overline{q}$, $b\overline{s}$, and $b\overline{q}$ with the principle quantum number n at a) $\alpha=\beta=1$. b) $\alpha=\beta=0.4$.

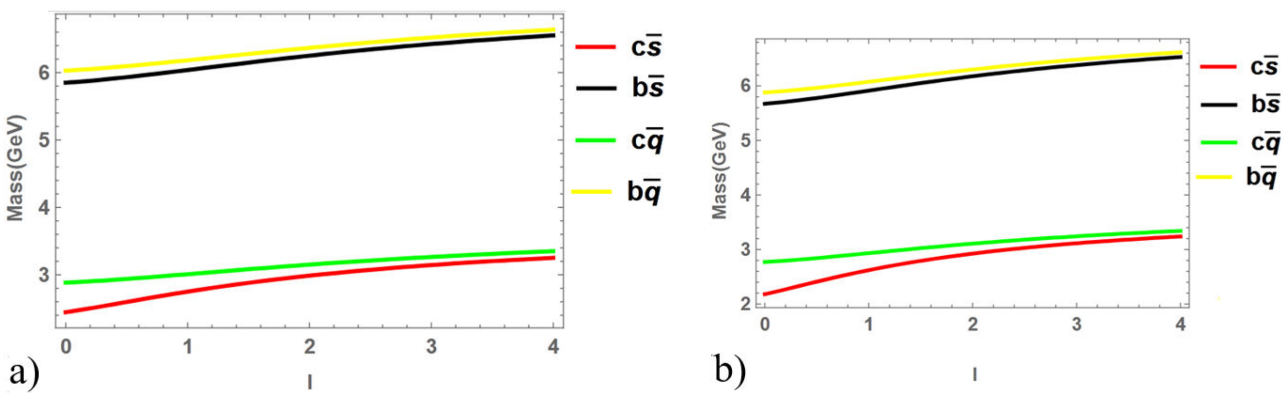

FIGURE 10. The mass spectra of $c\overline{s}$, $c\overline{q}$, $b\overline{s}$, and $b\overline{q}$ with the orbital angular momentum quantum number l at a) $\alpha=\beta=1$. b) $\alpha=\beta=0.4$.

4.3.1. Partition function

$$Z(\beta_s)=\int_0^{\lambda} e^{-\beta_s E_n}\,d\lambda, \tag{67}$$

$$\begin{aligned}Z(\beta_s)=&\frac{1}{\kappa\,\alpha}e^{\beta_s(-A_1-\frac{1}{2}A_2A_3)}\left(\frac{-1}{2\,\alpha\,\kappa\,\sqrt{-A_2\,\beta_s}}e^{\frac{-1}{2}\sqrt{-A_2\,\beta_s}\sqrt{-A_2A_3{}^2\,\beta_s}}\sqrt{\pi}\right)\\ &\times\left(e^{\sqrt{-A_2\,\beta_s}\sqrt{-A_2A_3{}^2\,\beta_s}}D-e^{\sqrt{-A_2\,\beta_s}\sqrt{-A_2A_3{}^2\,\beta_s}}B+F-M\right),\end{aligned} \tag{68}$$

$$D=Erfi\left(\frac{4\,A_4{}^2\sqrt{-A_2\,\beta_s}+\alpha^2\,\kappa^2\,\sqrt{-A_2\,\beta_s}+4\sqrt{-A_2A_3{}^2\,\beta_s}+\,4\,A_4\,\alpha\,\kappa\sqrt{-A_2\,\beta_s}}{8\,A_4+4\,\alpha\,\kappa}\right),$$

$$B=Erfi\left(\frac{4\,A_4{}^2\sqrt{-A_2\,\beta_s}+\alpha^2\,(\kappa+2\,\lambda\kappa)^2\,\sqrt{-A_2\,\beta_s}+4\sqrt{-A_2A_3{}^2\,\beta_s}+\,4\,A_4(1+2\,\lambda)\,\alpha\,\kappa\sqrt{-A_2\,\beta_s}}{8\,A_4+4(1+2\,\lambda)\,\alpha\,\kappa}\right), \tag{69}$$

$$F=Erfi\left(\frac{1}{4}(2\,A_4\sqrt{-A_2\,\beta_s}+\,\alpha\,\kappa\sqrt{-A_2\,\beta_s}-\frac{4\sqrt{-A_2A_3{}^2\,\beta_s}}{2\,A_4+\alpha\,\kappa})\right), \tag{70}$$

$$M=Erfi\left(\frac{1}{4}(2\,A_4\sqrt{-A_2\,\beta_s}+(1+2\,\lambda)\,\alpha\,\kappa\sqrt{-A_2\,\beta_s}-\frac{4\sqrt{-A_2A_3{}^2\,\beta_s}}{2\,A_4+\alpha\,\kappa\lambda})\right),$$

$$A_1=\frac{\rho^2}{2\,\mu}\left(t_3+\frac{1}{4}(k\alpha-1)^2\right),\qquad A_2=\frac{\rho^2}{2\,\mu},\qquad A_3=(t_1-t_3),\qquad A_4=\sqrt{\frac{1}{4}k^2\,\alpha^2\,+t_1-t_2+t_3}. \tag{71}$$

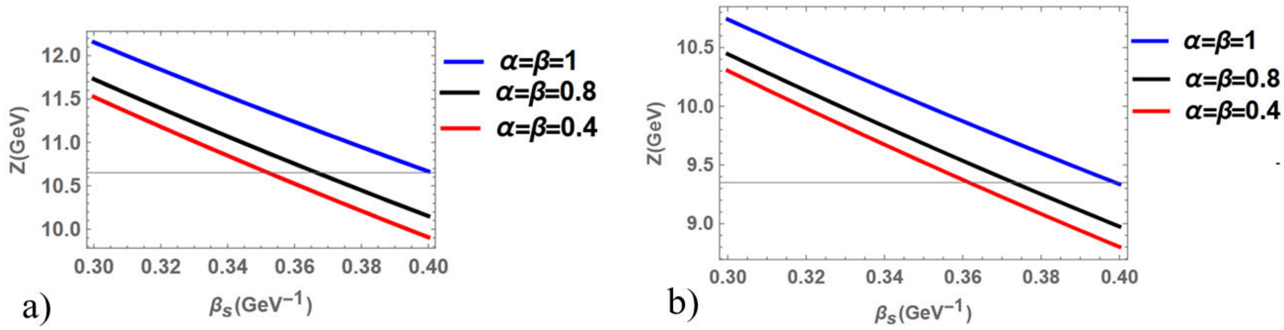

FIGURE 11. The partition function (Z) for $c\bar{s}$ is presented as a function of β_s, for various values of the fractional parameters α and β at (the orbital angular momentum quantum number a) $l = 0$, b) $l = 1$).

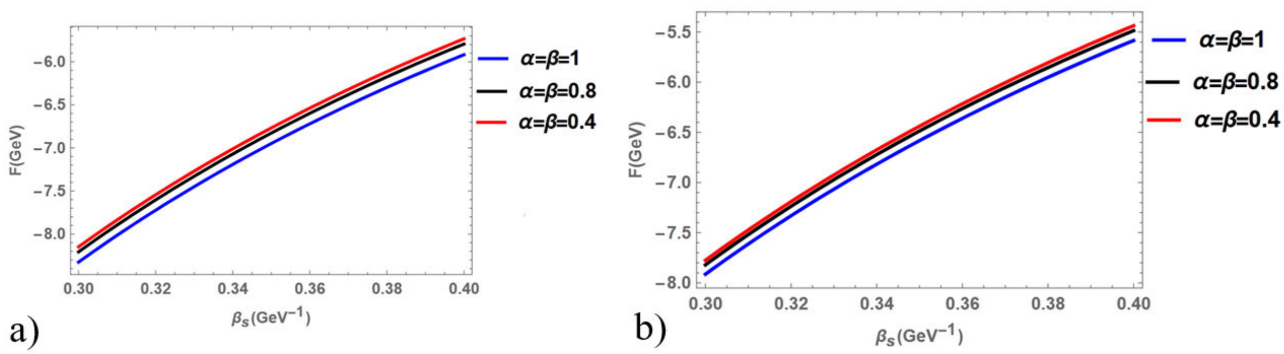

FIGURE 12. The free energy (F) for $c\bar{s}$ is presented as a function of β_s, for various values of the fractional parameters α and β at (the orbital angular momentum quantum number c) $l = 0$, d) $l = 1$).

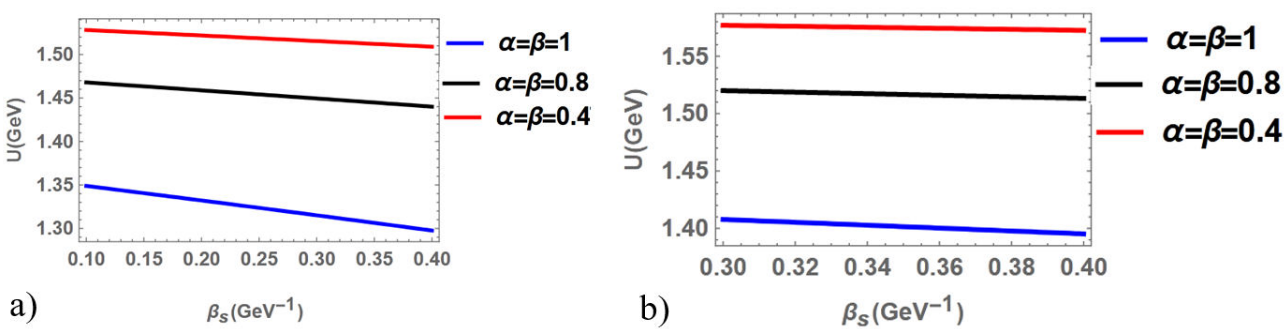

FIGURE 13. The mean energy (U) for $c\bar{s}$ is presented as a function of β_s, for various values of the fractional parameters α and β at (the orbital angular momentum quantum number a) $l = 0$, b) $l = 1$).

4.3.2. *Free energy F*

$$F(\beta_s) = -\frac{1}{\beta_s} \ln Z(\beta_s). \tag{72}$$

4.3.3. *Mean energy U*

$$U(\beta_s) = -\frac{\partial}{\partial(\beta_s)} \ln Z(\beta_s). \tag{73}$$

4.3.4. *Specific heat C*

$$C(\beta_s) = \frac{\partial(U)}{\partial T} = -K\, {\beta_s}^2 \frac{\partial(U)}{\partial(\beta_s)}. \tag{74}$$

4.3.5. *The entropy*

$$S(\beta_s) = K \ln Z(\beta_s) - K\, \beta_s \frac{\partial \ln Z(\beta_s)}{\partial \beta_s}. \tag{75}$$

In Fig. 11, we plot the partition function $Z(\beta_s)$ of cs^- as a function of β_s for various values of the fractional parameters α and β, under the influence of the orbital angular momentum quantum number l ((a) $l = 0$, (b) $l = 1$).

We observe that the partition function increases with rising values of α and β but decreases as l increases. Additionally, as β_s increases, $Z(\beta_s)$ decreases, consistent with Refs. [27, 61–63].

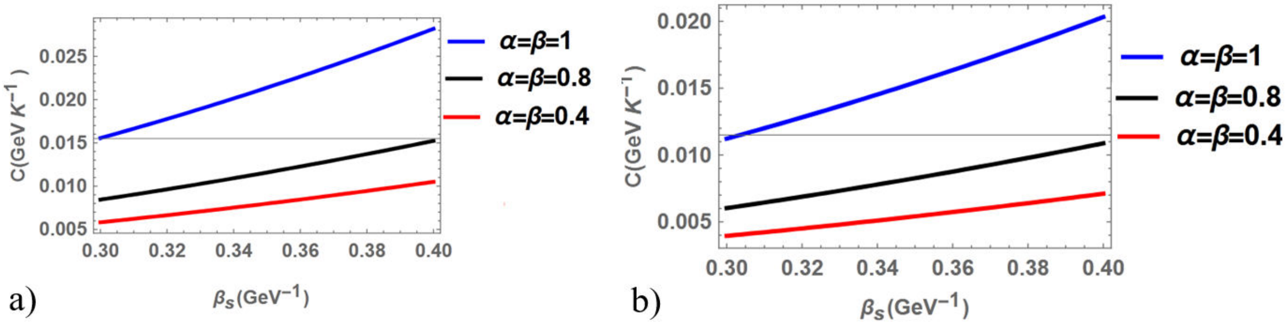

FIGURE 14. The specific heat for $c\overline{s}$ is presented as a function of β_s, for various values of the fractional parameters α and β at [the orbital angular momentum quantum number a) $l = 0$, b) $l = 1$].

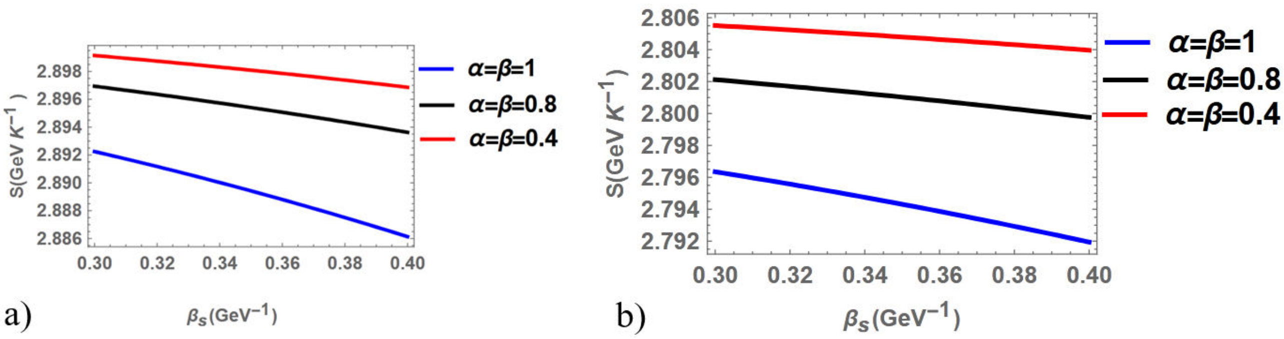

FIGURE 15. The entropy for $c\overline{s}$ is shown as a function of β_s, for different values of the fractional parameters α and β at [the orbital angular momentum quantum number a) $l = 0$, b) $l = 1$].

In Ref. [27], the authors used the generalized fractional extended NU method to solve the fractional Schrödinger equation (SE) with a harmonic oscillator potential. They found that as β_s increases, $Z(\beta_s)$ decreases, while higher values of α and β cause $Z(\beta_s)$ to increase.

Reference [61] analyzed the SE with a harmonic oscillator potential using the generalized Dunkl derivative in quantum mechanics, deriving energy eigenvalues and showing that the partition function decreases with β_s.

Similarly, Ref. [60] employed the DFDEP method with the NU approach to solve the Klein-Gordon equation and found that $Z(\beta_s)$ decreases as β_s increases. Ref. [63] studied the thermodynamic properties of heavy mesons using the N-dimensional SE with an expanded Cornell potential and also reported that $Z(\beta_s)$ decreases with β_s.

In Fig. 12, the free energy F of cs^- is plotted as a function of β_s [a) $l = 0$, b) $l = 1$] for various values of α and β.

The results show that F increases with higher α and β values, while it decreases with increasing l.

Additionally, as β_s increases, F increases, but F decreases as temperature rises, consistent with Refs. [27, 62–65].

Reference [64] computed the phase diagram and thermodynamic properties of quark-gluon plasma (QGP) as functions of temperature and baryon density, considering weakly interacting light quarks and gluons.

Reference [65] used a density- and temperature-dependent potential model to calculate the thermodynamic parameters of quark matter, showing similar trends in free energy behavior.

In Fig. 13, we plot the mean energy U of cs^- as a function of β_s [a) $l = 0$, b) $l = 1$] for different α and β values. We observe that U decreases with increasing α and β. As β_s increases, Ualso declines.

Furthermore, U increases with higher l, consistent with Refs. [27, 61–63].

In Fig. 14, the specific heat C of cs^- is plotted as a function of β_s [a) $l = 0$, b) $l = 1$] for various α and β values. The specific heat increases with β_s, consistent with Ref. [27, 66].

However, C decreases with higher values of l. In Fig. 15, the entropy S of cs^- is displayed as a function of β_s [a) $l = 0$, b) $l = 1$] for various α and β values.

We find that S decreases as α and β increase. Moreover, S declines with β_s and decreases further with higher l. These results are consistent with Refs. [27, 61, 63, 66].

5. Conclusion

In this study, we applied the Yukawa potential model and the screened modified Kratzer potential to solve the generalized fractional Klein-Gordon equation using the generalized fractional parametric NU method.

For both relativistic and non-relativistic cases, we derived the generalized fractional energy eigenvalues and wave functions, comparing the results with previous studies. For the non-relativistic case, we calculated the masses of heavy and heavy-light mesons.

The use of the generalized fractional derivative proved essential, as it reduced the total error in calculating these masses. This novel approach provides a highly accurate method for determining the masses of charmonium and bottomonium mesons in various excited states, achieving excellent agreement with experimental data and significantly reducing error rates compared to earlier methods [7,30,31,44–47,49–57,59,60].

We also analyzed the thermodynamic properties of the heavy-light meson cs^- graphically. The partition function $Z(\beta_s)$ was found to increase with rising values of α and β but decreases as l increases. As (β_s) grows, $Z(\beta_s)$ decreases, aligning with results from previous studies [27,61–63].

The free energy F increases with (β_s) but decreases as temperature rises, contrasting with results in Refs. [27,62–65].

Additionally, increasing l leads to a decrease in free energy. For the mean energy U of cs^-, as a function of (β_s), the results show that increasing α and β lowers the curve. Similarly, as (β_s) increases, U decreases, which agrees with Refs. [27,61–63].

Increasing l also reduces the mean energy. The specific heat of cs^- was plotted as a function of $(\beta_s)$for different values of α and β.

The results indicate that higher α and β values lead to higher specific heat, which also increases with (β_s), consistent with Ref. [27,66].

However, increasing l decreases the specific heat. Finally, the entropy was observed to decrease with (β_s) , aligning with Ref. [27,59,61,64], and it also decreases as l increases.

1. L.-Z. Yi *et al.*, Bound states of the Klein–Gordon equation with vector and scalar Rosen–Morse-type potentials. *Physics Letters A* **333** (2004) 212. `https://doi.org/10.1016/j.physleta.2004.10.054`.
2. X.-C. Zhang *et al.*, Bound states of the Dirac equation with vector and scalar Scarf-type potentials. *Physics Letters A* **340** (2005) 59. `https://doi.org/10.1016/j.physleta.2005.04.011`.
3. K. K. Likharev, *Quantum Mechanics: Lecture notes: Lecture notes*. (IOP Publishing, 2019).
4. S. Dong, and M. Lozada-Cassou. Exact solutions of the Klein-Gordon equation with scalar and vector ring-shaped potentials. *Physica Scripta* **74** (2006) 285, `https://doi.org/10.1088/0031-8949/74/2/024`.
5. P. Alberto, A. S. de Castro, and M. Malheiro. Spin and pseudospin symmetries and the equivalent spectra of relativistic spin-1/2 and spin-0 particles. *Physical Review C-Nuclear Physics* **75** (2007) 047303, `https://doi.org/10.1103/PhysRevC.75.047303`.
6. E. S. William, E. P. Inyang, and E. A. Thompson *Rev. Mex. Fis.* **66** (2020) 730, `https://doi.org/10.31349/revmexfis.66.730`.
7. E. P. Inyang *et al.*, Approximate solutions of D-dimensional Klein–Gordon equation with Yukawa potential via Nikiforov–Uvarov method. *Indian Journal of Physics* **95** (2021) 2733, `https://doi.org/10.1007/s12648-020-01933-x`.
8. C. Berkdemir, A. Berkdemir, and J. Han, Bound state solutions of the Schr odinger equation for modified Kratzer's molecular potential. *Chemical Physics Letters* **417** (2006) 326, `https://doi.org/10.1016/j.cplett.2005.10.039`.
9. E. Inyang, and E. Obisung, The study of electronic states of NI and ScI molecules with screened Kratzer Potential. *East European Journal of Physics* **3** (2022) 32, `https://doi.org/10.26565/2312-4334-2022-3-04`.
10. E. P. Inyang *et al.*, Quark-antiquark study with inversely quadratic yukawa potential using the nikiforov-uvarov-functional-analysis method. *East European Journal of Physics* **2** (2022) 43, `https://doi.org/10.26565/2312-4334-2022-2-05`.
11. A. Kratzer, Die ultraroten rotationsspektren der halogenwasserstoffe. *Zeitschrift f ur Physik* **3** (1920) 289, `https://doi.org/10.1007/bf01327754`.
12. A. N. Ikot *et al.*, Eigensolution, expectation values and thermodynamic properties of the screened Kratzer potential. *The European Physical Journal Plus* **134** (2019) 386, `https://doi.org/10.1140/epjp/i2019-12783-x`.
13. C. O. Edet *et al.*, Eigenfunctions, uncertainties and thermal properties of diatomic molecules under screened modified Kratzer potential. *Indian Journal of Physics* **96** (2022) 3429, `https://doi.org/10.1007/s12648-022-02292-5`.
14. E. P. Inyang *et al.*, Masses and thermodynamic properties of a Quarkonium system. *Canadian Journal of Physics* **99** (2021) 982, `https://doi.org/10.1139/cjp-2020-0578`.
15. E. P. Inyang *et al.*, Energy spectra and expectation values of selected diatomic molecules through the solutions of Klein–Gordon equation with Eckart–Hellmann potential model. *Molecular Physics* **119** (2021) e1956615, `https://doi.org/10.1080/00268976.2021.1956615`.
16. E. P. Inyang *et al.*, Masses and thermal properties of a charmonium and Bottomonium mesons. *Journal of the Nigerian Society of Physical Sciences* (2022) 884.
17. E. P. Inyang *et al.*, Investigation of quantum information theory with the screened modified Kratzer and a class of Yukawa potential model. *The European Physical Journal Plus* **138** (2023) 969, `https://doi.org/10.1140/epjp/s13360-023-04617-7`.
18. A. D. Antia, I. Okon Akpan, and A. Okon Akankpo, Relativistic treatment of spinless particles subject to modified Scarf II potential. *International Journal of High Energy Physics*

2 (2015) 50, https://doi.org/10.11648/j.ijhep.20150204.12.

19. H. Hassanabadi, S. Zarrinkamar, and A. A. Rajabi, Exact solutions of D-dimensional Schr odinger equation for an energy-dependent potential by NU method. *Communications in Theoretical Physics* **55** (2011) 541, https://doi.org/10.1088/0253-6102/55/4/01.
20. M. Safi Ullah, and M. Zulfikar Ali, Bifurcation analysis and new waveforms to the fractional KFG equation. *Partial Differential Equations in Applied Mathematics* **10** (2024) 100716, https://doi.org/10.1016/j.padiff.2024.100716.
21. H. H. Karayer, A.D. Demirhan, F. Büyükkılıç, *Turk. J. Phys.* **41** (2017) 551, https://doi.org/10.3906/fiz-1707-9.
22. M. Abu-Shady, and M. K. A. Kaabar, A generalized definition of the fractional derivative with applications. *Mathematical problems in engineering* **2021** (2021) 9444803, https://doi.org/10.1155/2021/9444803.
23. G. Jumarie, Modified Riemann-Liouville derivative and fractional Taylor series of nondifferentiable functions further results. *Computers & Mathematics with Applications* **51** (2006) 1367, https://doi.org/10.1016/j.camwa.2006.02.001.
24. M. Abu-Shady, and Sh Y. Ezz-Alarab. Conformable fractional of the analytical exact iteration method for heavy quarkonium masses spectra. *Few-Body Systems*, **62** (2021) 1-8.
25. M. Caputo, Linear Models of Dissipation whose Q is almost Frequency Independent- II. *Geophysical. J. Int.* **13** (1967) 529, https://doi.org/10.1111/j.1365-246X.1967.tb02303.x.
26. R. Khalil *et al*., A new definition of fractional derivative. *Journal of computational and applied mathematics* **264** (2014) 65, https://doi.org/10.1016/j.cam.2014.01.002.
27. M. Abu-shady, and H. M. Fath-Allah, Properties and behaviors of heavy quarkonia: insights through fractional model and topological defects. *Advances in High Energy Physics* **2024** (2024) 2730568, https://doi.org/10.1155/2024/2730568.
28. A. N. Ikot *et al*., Relativistic and non-relativistic thermal properties with bound and scattering states of the Klein-Gordon equation for Mobius square plus generalized Yukawa potentials. *Indian Journal of Physics* **97** (2023) 2871, https://doi.org/10.1007/s12648-023-02654-7.
29. E. P. Inyang *et al*., Masses and thermal properties of a charmonium and Bottomonium mesons. *Journal of the Nigerian Society of Physical Sciences* (2022) 884.
30. R. Kumar and F. Chand, Asymptotic study to the N-dimensional radial Schr odinger equation for the quark-antiquark system, *Communications in Theoretical Physics*, **59** (2013) 528, https://doi.org/10.1088/0253-6102/59/5/02.
31. R. Rani, S. B. Bhardwaj, and Fakir Chand, Mass spectra of heavy and light mesons using asymptotic iteration method. *Communications in Theoretical Physics* **70** (2018) 179, https://doi.org/10.1088/0253-6102/70/2/179.
32. D. Molina *et al*., Bottomonium spectrum with a Dirac potential model in the momentum space. *The European Physical Journal C* **80** (2020) 526, https://doi.org/10.1140/epjc/s10052-020-8099-z.
33. T. Barnes, S. Godfrey, and E. S. Swanson, Higher charmonia. *Physical Review D—Particles, Fields, Gravitation, and Cosmology* **72** (2005) 054026, https://doi.org/10.1103/PhysRevD.72.054026.
34. M. Schleif and R. W unsch, Thermodynamic properties of the SU(2) f chiral quark–loop soliton, *The European Physic Journal A-Hadrons and Nuclei*, **1** (1998) 171, https://doi.org/10.1007/s100500050046.
35. M. Abu-Shady, Meson properties at finite temperature in the linear sigma model, *International Journal of Theoretical Physics*, **49** (2010) 2425, https://doi.org/10.1007/s10773-010-0428-9.
36. M. Abu-Shady, The effect of finite temperature on the nucleon properties in the extended linear sigma model. *International Journal of Modern Physics E* **21** (2012) 1250061, https://doi.org/10.1142/S0218301312500619.
37. M. Abu-Shady, E. M. Khokha, and T. A. Abdel-Karim. The generalized fractional NU method for the diatomic molecules in the Deng-Fan model. *The European Physical Journal D* **76** (2022) 159.
38. A. F. Nikiforov, V. B. Uvarov, Special Functions of Mathematical Physics. Birkh auser, (Basel 1988).
39. M. Abu-shady, and H. M. Fath-Allah. The Parametric Generalized Fractional Nikiforov-Uvarov Method and Its Applications. *East European Journal of Physics*. **3** (2023) 248, https://doi.org/10.26565/2312-4334-2023-3-22.
40. C. Tezcan, and R. Sever, A general approach for the exact solution of the Schrödinger equation. *International Journal of Theoretical Physics* **48** (2009) 337, https://doi.org/10.1007/s10773-008-9806-y.
41. W. Greiner, Relativistic quantum mechanics. Vol. 2. (springer, Berlin, 2000).
42. R. L. Greene, and C. Aldrich. Variational wave functions for a screened Coulomb potential. *Physical Review A* **14** (1976) 2363, https://doi.org/10.1103/PhysRevA.14.2363.
43. M. Tanabashi, C. D. Carone, T. G. Trippe and C. G. Wohl *Phys. Rev. D* **98** (2018) 548.
44. E. E. Ibekwe *et al*., Bound state solution of radial schrodinger equation for the quark–antiquark interaction potential. *Iranian Journal of Science and Technology, Transactions A: Science* **44** (2020) 1191, https://doi.org/10.1007/s40995-020-00913-4.
45. E. Omugbe, E. Omosede Osafile, and M. C. Onyeaju, Mass spectrum of mesons via the WKB approximation method. *Advances in High Energy Physics* **2020** (2020) 5901464, https://doi.org/10.1155/2020/5901464.
46. M. Abu-Shady, N-dimensional Schrödinger equation at finite temperature using the Nikiforov-Uvarov method. *Journal of the Egyptian mathematical society* **25** (2017) 86, https://doi.org/10.1016/j.joems.2016.06.006.

47. R. Kumar, and F. Chand, Series solutions to the N-dimensional radial Schrödinger equation for the quark–antiquark interaction potential. *Physica Scripta* **85** (2012) 055008, https://doi.org/10.1088/0031-8949/85/05/055008.

48. M. Tanabashi *et al*., Review of particle physics. *Physical Review D* **98** (2018).

49. M. Abu-Shady, and Sh. Y. Ezz-Alarab, Trigonometric Rosen–Morse potential as a quark–antiquark interaction potential for meson properties in the non-relativistic quark model using EAIM. *Few-body systems* **60** (2019) 66, https://doi.org/10.1007/s00601-019-1531-y.

50. D. Ebert, R. N. Faustov, and V. O. Galkin. Heavy-light meson spectroscopy and Regge trajectories in the relativistic quark model. *The European Physical Journal C* **66** (2010) 197, https://doi.org/10.1140/epjc/s10052-010-1233-6.

51. M. Abu-Shady, and E. M. Khokha. Bound state solutions of the Dirac equation for the generalized Cornell potential model. *International Journal of Modern Physics A* **36** (2021) 2150195, https://doi.org/10.1142/S0217751X21501955.

52. K. R. Purohit, A. Kumar Rai, and R. H. Parmar, Spectroscopy of heavy-light mesons ($\mathrm{c}\bar{\mathrm{s}}$, $\mathrm{c}\bar{\mathrm{q}}$, $\mathrm{b}\bar{\mathrm{s}}$, $\mathrm{b}\bar{\mathrm{q}}$) for the linear plus modified Yukawa potential using Nikiforov-Uvarov method. *Indian Journal of Physics* **98** (2024) 1109, https://doi.org/10.1007/s12648-023-02852-3.

53. J.-B. Liu, and C.-D. Lü, Spectra of heavy–light mesons in a relativistic model. *The European Physical Journal C* **77** (2017) 312, https://doi.org/10.1140/epjc/s10052-017-4867-9.

54. M. Shah, B. Patel, and P. C. Vinodkumar, Spectroscopy and flavor changing decays of B, B s mesons in a Dirac formalism. *Physical Review D* **93** (2016) 094028, https://doi.org/10.1103/PhysRevD.93.094028.

55. V. Patel, R. Chaturvedi, and A. K. Rai, Spectroscopic properties of D-meson using screened potential. *The European Physical Journal Plus* **136** (2021) 42, https://doi.org/10.1140/epjp/s13360-020-01039-7.

56. S. Godfrey, and K. Moats, Properties of excited charm and charm-strange mesons. Physical Review D **93** (2016) 034035, https://doi.org/10.1103/PhysRevD.93.034035.

57. N. Devlani, and A. Kumar Rai, Mass spectrum and decay properties of D meson. *International Journal of Theoretical Physics* **52** (2013) 2196, https://doi.org/10.1007/s10773-013-1494-6.

58. C. Patrignani, Review of particle physics. *Chinese Physics C* **40** (2016) 100001. https://doi.org/10.1088/1674-1137/40/10/100001.

59. V. Patel, R. Chaturvedi, and A. Kumar Rai, Spectroscopic properties of B and B_s meson using screened potential. *Indian Journal of Physics* (2024) 1, https://doi.org/10.1007/s12648-023-03048-5.

60. S. Godfrey, Kenneth Moats, and E. S. Swanson. B and B s meson spectroscopy. *Physical Review D* **94** (2016) 054025, https://doi.org/10.1103/PhysRevD.94.054025.

61. S. H. Dong, W. H. Huang, W. S. Chung, P. Sedaghatnia, and H. Hassanabadi, Exact solutions to generalized Dunkl oscillator and its thermodynamic properties, *Euro physics Letters* **135** (2021) 30006, https://doi.org/10.1209/0295-5075/ac2453.

62. A. N. Ikot, B. C. Lutfuoglu, M. I. Ngwueke, M. E. Udoh, S. Zare, and H. Hassanabadi, Klein-Gordon equation particles in exponential-type molecule potentials and their thermodynamic properties in D dimensions, *The European Physic Journal Plus*, **131** (2016) 419, https://doi.org/10.1140/epjp/i2016-16419-5.

63. M. Abu-Shady, T. A. Abdel-Karim, and Sh Y. Ezz-Alarab. Masses and thermodynamic properties of heavy mesons in the non-relativistic quark model using the Nikiforov–Uvarov method. *Journal of the Egyptian Mathematical Society* **27** (2019) 14, https://doi.org/10.1186/s42787-019-0014-0.

64. M. Modarres and A. Mohamadnejad, The thermodynamic properties of weakly interacting quark-gluon plasma via the one-gluon exchange interaction, *Physics of Particles and Nuclei Letters*, **10** (2013) 99, https://doi.org/10.1134/S1547477113020106.

65. M. Modarres and H. Gholizade, Strange quark matter in the framework of one gluon exchange and density and temperature dependent particle mass models, *International Journal of Modern Physics E*, **17** (2008) 1335, https://doi.org/10.1142/S0218301308010453.

66. C. O. Edet *et al*., Magneto-transport and thermal properties of the Yukawa potential in cosmic string space-time, *Results in Physics*, **39** (2022) 105749, https://doi.org/10.1016/j.rinp.2022.105749.